ORGANIC LETTERS

XXXX
Vol. XX, No. XX
000–000

Synthesis and Reduction Kinetics of Sterically Shielded Pyrrolidine Nitroxides

Joseph T. Paletta,[†] Maren Pink,[‡] Bridget Foley,[†] Suchada Rajca,[†] and Andrzej Rajca*[,†]

Department of Chemistry, University of Nebraska, Lincoln, Nebraska 68588-0304, United States, and IUMSC, Department of Chemistry, Indiana University, Bloomington, Indiana 47405-7102, United States

arajca1@unl.edu

Received September 11, 2012

ABSTRACT

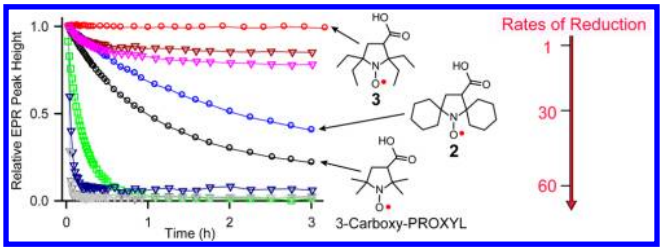

A series of sterically shielded pyrrolidine nitroxides were synthesized, and their reduction by ascorbate (vitamin C) indicate that nitroxide 3, a tetraethyl derivative of 3-carboxy-PROXYL, is reduced at the slowest rate among known nitroxides, i.e., at a 60-fold slower rate than that for 3-carboxy-PROXYL.

Nitroxide radicals have a wide range of applications in organic synthesis,[1] materials chemistry,[2,3] biophysics,[4] and biomedicine.[5] These applications rely on the stability, paramagnetic properties,[6] and/or redox properties[7] of the radicals at ambient conditions. While fast redox reactions of nitroxide radicals are favorable for many applications, fast *in vivo* reduction of paramagnetic nitroxide radicals to diamagnetic hydroxylamines by antioxidants, such as ascorbate (vitamin C) or enzymatic systems, hinders their applications in biomedicine.

3-Carboxy-PROXYL (**1**) (Figure 1) and its carboxylic acid derivatives are among the most commonly used nitroxides *in vivo* because of their resistance to reduction.[9] However, their half-life is only ~2 min in the bloodstream and major organs, as determined by magnetic resonance imaging (MRI) studies in mice.[9] Therefore, their applications as paramagnetic contrast agents in MRI or *in vivo* spin labels are rather limited.[10]

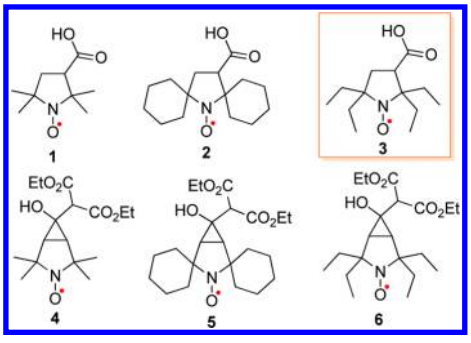

Figure 1. Pyrrolidine nitroxides.

[†] University of Nebraska.
[‡] Indiana University.

(1) Tebben, L.; Studer, A. *Angew. Chem., Int. Ed.* **2011**, *50*, 5034–5068.
(2) (a) Ratera, I.; Veciana *J. Chem. Soc. Rev.* **2012**, *41*, 303–349. (b) Lahti, P. M. *Adv. Phys. Org. Chem.* **2011**, *45*, 93–169.
(3) Nishide, H.; Oyaizu, K. *Science* **2008**, *319*, 737–738.
(4) Reginsson, G. W.; Schiemann, O. *Biochem. J.* **2011**, *434*, 353–363.
(5) Burks, S. R.; Makowsky, M. A.; Yaffe, Z. A.; Hoggle, C.; Tsai, P.; Muralidharan, S.; Bowman, M. K.; Kao, J. P. Y.; Rosen, G. M. *J. Org. Chem.* **2010**, *75*, 4737–4741.
(6) (a) Dane, E. L.; Griffin, R. G.; Swager, T. M. *Org. Lett.* **2009**, *11*, 1871–1874. (b) Rajca, A.; Mukherjee, S.; Pink, M.; Rajca, S. *J. Am. Chem. Soc.* **2006**, *128*, 13497–13507. (c) Olankitwanit, A.; Kathirvelu, V.; Rajca, S.; Eaton, G. R.; Eaton, S. S.; Rajca, A. *Chem. Commun.* **2011**, *47*, 6443–6445. (d) Zagdoun, A.; Casano, G.; Ouari, O.; Lapadula, G.; Rossini, A. J.; Lelli, M.; Baffert, M.; Gajan, D.; Veyre, L.; Maas, W. E.; Rosay, M.; Weber, R. T.; Thieuleux, C.; Coperet, C.; Lesage, A.; Tordo, P.; Emsley, L. *J. Am. Chem. Soc.* **2012**, *134*, 2284–2291.
(7) (a) Oyaizu, K.; Nishide, H. *Adv. Mater.* **2009**, *21*, 2339–2344. (b) Gryn'ova1, G.; Barakat, J. M.; Blinco, J. P.; Bottle, S. E.; Coote, M. L. *Chem.—Eur. J.* **2012**, *18*, 7582–7593.
(8) Keana, J. F. W.; Pou, S.; Rosen, G. M. *Magn. Res. Med.* **1987**, *5*, 525–536.
(9) Hyodo, F.; Matsumoto, K.; Matsumoto, A.; Mitchell, J. B.; Krishna, M. C. *Cancer Res.* **2006**, *66*, 9921–9928.
(10) (a) Davis, R. M.; Sowers, A. L.; DeGraff, W.; Bernardo, M.; Thet-ford, A.; Krishna, M. C.; Mitchell, J. B. *Free Radical Biol. Med.* **2011**, *51*, 780–790. (b) Khan, N.; Blinco, J. P.; Bottle, S. E.; Hosokawa, K.; Swartz, H. M.; Micallef, A. S. *J. Magn. Reson.* **2011**, *211*, 170–177.

10.1021/ol302506f © XXXX American Chemical Society

Recently, we reported the design and synthesis of an MRI contrast agent based upon macromolecular polyradicals derived from spirocyclohexyl nitroxide **2** (Figure 1).[11,12] The agent possesses a comparatively long *in vivo* lifetime and high ^{1}H water relaxivity (r_1) and provides contrast-enhanced high resolution MRI in mice for over 1 h.[11]

To further improve the development of organic based MRI contrast agents, we explore nitroxides that are more resistant to reduction than **2**. It is well-established that the slower rate of reduction of nitroxides is associated with ring size, i.e. five-membered (pyrrolidine) vs six-membered (piperidine) ring structures,[9] as well as steric shielding of the nitroxide moiety.[13,14] To search for nitroxides with increased resistance to reduction, we focus on a series of sterically shielded pyrrolidine nitroxides and their rate of reduction with ascorbate. Typically, the rate of reduction of a nitroxide by ascorbate *in vitro* provides a qualitative guideline to its expected half-life *in vivo*.[11,14]

Herein we report the synthesis of sterically shielded pyrrolidine nitroxides **3**–**6** (Figure 1) and reduction kinetics of nitroxides **1**–**6** by ascorbate.

Scheme 1. Synthesis of Nitroxides **3** and **3**-NHS[a]

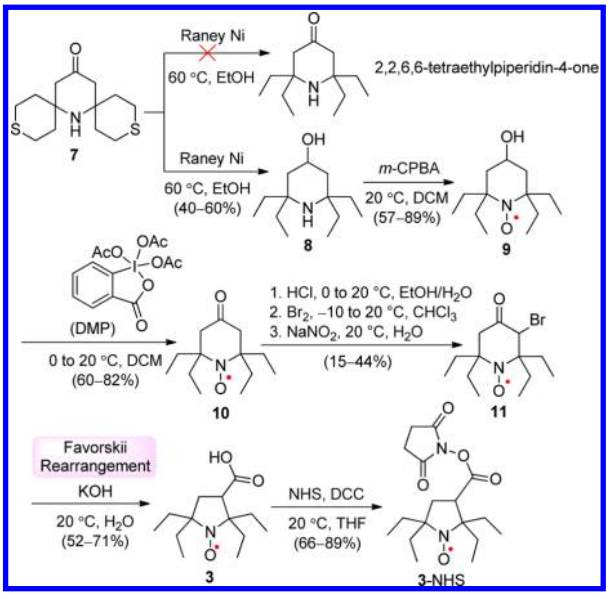

[a] Isolated yields.

Synthesis of nitroxide **3** is outlined in Scheme 1. Starting from **7**, we followed the desulfurization procedure using Raney Ni, which was previously reported to provide 2,2,6,6-tetraethylpiperidine-4-one in 15% yield.[15] However, we found that the major product was alcohol **8**,[16] which could be obtained in about 50% yield using a larger excess of Raney Ni. We expected that, under similar conditions for the preparation of Tempone (**16**),[17] oxidation of **8** using *m*-CPBA would provide **10**. Instead, we obtained **9**,[16] which was then oxidized further with Dess–Martin periodinane (DMP) to give ketone-nitroxide **10**. By adapting the previously reported procedure for bromination of Tempone,[18] **11** was obtained by protonation of nitroxide **10**, followed by bromination, and recovery of nitroxide with sodium nitrite. Nitroxide **11** in potassium hydroxide solution at 20 °C undergoes Favorskii rearrangement[18] to give the target nitroxide **3**. Treatment of **3** with *N*-hydroxysuccinimide (NHS) and *N*,*N*′-dicyclohexylcarbodiimide (DCC) in THF provides spin label **3**-NHS in good yield.

The synthesis of bicyclic pyrrolidine nitroxides is based on partial Favorskii rerrangement of **12** leading to **4**.[19] Sodium diethyl malonate is added to a solution of a bromoketone in anhydrous THF, and then the reaction mixture is stirred at 50 °C for 1.5–2.5 h, to produce bicyclic nitroxides **4**–**6** in about 50% isolated yields as mixtures of diastereomers (Scheme 2).

Scheme 2. Synthesis of Nitroxides **4**–**6**

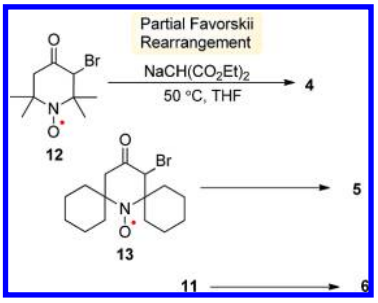

Structures of nitroxides **2** and **3** are confirmed by single-crystal X-ray analysis (Figure 2).[20]

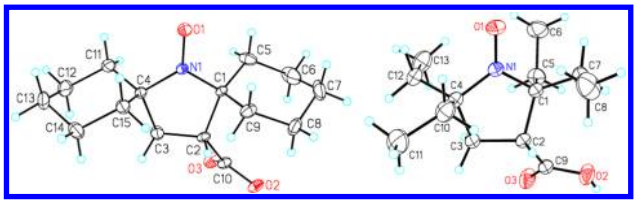

Figure 2. X-ray structures for nitroxide radicals **2** (left) and **3** (right). Carbon, nitrogen, and oxygen atoms are depicted with thermal ellipsoids set at the 50% probability level.

(11) Rajca, A.; Wang, Y.; Boska, M.; Paletta, J. T.; Olankitwanit, A.; Swanson, M. A.; Mitchell, D. G.; Eaton, S. S.; Eaton, G. R.; Rajca, S. *J. Am. Chem. Soc.* **2012**, *134*, 15724–15727.

(12) Kirilyuk, I. A.; Polienko, Y. F.; Krumkacheva, O. A.; Strizhakov, R. K.; Gatilov, Y. V.; Grigor'ev, I. A.; Bagryanskaya, E. G. *J. Org. Chem.* **2012**, *77*, 8016–8027.

(13) (a) Marxa, L.; Chiarellia, R.; Guiberteaub, T.; Rassat, A. *J. Chem. Soc., Perkin Trans. 1* **2000**, 1181–1182. (b) Bobko, A. A.; Kirilyuk, I. A.; Grigor'ev, I. A.; Zweier, J. L.; Khramtsov, V. V. *Free Radical Biol. Med.* **2007**, *42*, 404–412.

(14) Emoto, M.; Mito, F.; Yamasaki, T.; Yamada, K.; Sato-Akaba, H.; Hirata, H.; Fujii, H. *Free Radical Res.* **2011**, *45*, 1325–1332.

(15) Sakai, K.; Yamada, K.; Yamasaki, T.; Kinoshita, Y.; Mito, F.; Utsumi, H. *Tetrahedron* **2010**, *66*, 2311–2315.

(16) Wetter, C.; Gierlich, J.; Knoop, C. A.; Müller, C.; Schulte, T.; Studer, A. *Chem.—Eur. J.* **2004**, *10*, 1156–1166.

(17) Cella, J. A.; Kelley, J. A.; Kenehan, E. F. *J. Chem. Soc., Chem. Commun.* **1974**, 943–943.

(18) Sosnovsky, G.; Cai, Z. *J. Org. Chem.* **1995**, *60*, 3414–3418.

Table 1. Second-Order Rate Constants, k ($M^{-1}s^{-1}$), for Initial Rates of Reduction of Nitroxides (0.04−0.2 mM) with 20-Fold Excess Ascorbate in 25 mM PBS pH 7.4 at 295 K[a]

pyrrolidine nitroxides		piperidine nitroxides	
	k		k
1	0.063 ± 0.002	**14**	5.6 ± 0.2
2	0.031 ± 0.003	**15**	2.57 ± 0.03
3	≤0.001[b]	**9**	0.039 ± 0.003
4	0.354 ± 0.006	**16**	6.32 ± 0.01
5	0.170 ± 0.004	**17**	3.2 ± 0.2
6	0.01	**10**	0.044 ± 0.002

[a] Mean ± two standard deviations from at least three measurements; see: Tables S5−S6 in the SI. [b] 1 mM **3** with 20 or 100 mM ascorbate in 125 mM PBS.

The high purity of the bulk samples of nitroxides **3**−**6**, as well as all other nitroxides used for kinetic studies, is determined by paramagnetic ^{1}H NMR spectra and EPR spectroscopic spin concentrations.

EPR spectra of nitroxides **3**−**6** in chloroform show triplet patterns due to ^{14}N hyperfine splitting, $a_N \approx 14-16$ G, and g-values of about 2.006, similar to those for **1** and **2**. For bicylic nitroxide **4**, each of the triplet peaks is resolved into nonets, corresponding to the coupling of eight protons with ^{1}H hyperfine splitting, $a_H \approx 0.5$ G. This EPR splitting pattern is reproduced by DFT calculations,[21] using simplified structures for *cis* and *trans* diastereomers, in which the diethylmalonate moiety is replaced with a methyl group. Specifically, each diastereomer has eight protons with computed $a_H \approx 0.5$ G, i.e., two protons at the bridghead and six protons in the methyls that are *syn* to the cyclopropane moiety.[22]

Rates of reduction for pyrrolidine nitroxides **1**−**6** are studied under pseudo-first-order conditions using a 20-fold excess of ascorbate in pH 7.4 PBS buffer. For comparison, the rates of reduction of the *gem*-dimethyl, spirocyclohexyl, and *gem*-diethyl piperidine nitroxides **9**, **10**, **14**−**17**[9,14,23] are measured under identical conditions. Second-order rate constants, k, are obtained by monitoring the decay of the low-field EPR peak height of nitroxides at 295 K (Figure 3 and Table 1). Also, decays of EPR single integrated peak height are examined and found to produce similar values of k for most nitroxides (Tables S5 and S6, Supporting Information (SI)).

The values of k for *gem*-dimethyl nitroxides **1**, **14**, and **16** in Table 1, which may be compared to the corresponding k = 0.06, 5.46, 5.78 M^{-1} s^{-1} at 293 K reported by Rigo,[23] reflect a well-known finding that five-membered ring nitroxides are reduced at relatively slower rates, compared to six-membered ring nitroxides. The *gem*-dimethyl bicyclic

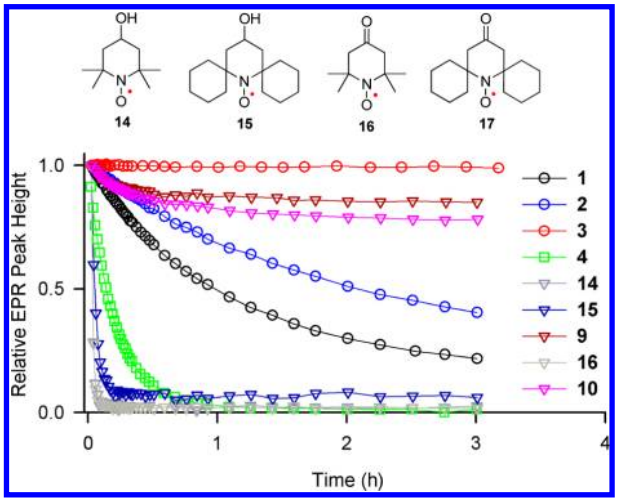

Figure 3. Reduction profiles of 0.2 mM nitroxides with 4 mM ascorbate in 25 mM PBS pH 7.4 at 295 K (**5**, **6**, and **17** have insufficient solubility to be included in the plot).

nitroxide **4** (k = 0.354 M^{-1} s^{-1}) is reduced at a significantly faster rate than **1** (Figure 3). The spirocyclohexyl nitroxides **2**, **5**, **15**, and **17** are reduced at rates that are about two times slower than those for the corresponding *gem*-dimethyl nitroxides. The rates of reduction for *gem*-diethyl nitroxides **3**, **6**, **9**, and **10** are decreased by another factor of 20−70, compared to the spirocyclohexyl nitroxides.

gem-Diethyl pyrrolidine nitroxides **3** ($k \leq 0.001$ M^{-1} s^{-1}) and **6** ($k \approx 0.01$ M^{-1} s^{-1}) are reduced at significantly slower rates, compared to previously reported nitroxides, including five-membered ring nitroxides shielded with *gem*-diethyl groups, such as 3,4-dimethyl-2,2,5,5-tetraethylperhydroimidazol-1-yloxy (k = 0.02 M^{-1} s^{-1}).[13b] As illustrated in Figure 3, 0.2 mM nitroxide **3** in the presence of a 20-fold excess of ascorbate shows no detectable decay over 3 h. Only when much higher concentrations of **3** and ascorbate are used, the reduction becomes detectable (Figure 4); for 1 mM **3** treated with 20 and 100 mM ascorbate, the EPR signal of nitroxide **3** decreases by only 5 and 15%, respectively, after 3 h.

The reduction profiles (Figure 4) suggest that the slow rate at the initial stage of the reaction ($k \approx 0.001$ M^{-1} s^{-1}, Table 1) is followed by slower decay of the EPR signal in the later stage. This observation may be interpreted as the initial slow reaction of ascorbate with nitroxide, which produces hydroxylamine and the ascorbate radical, reaching an "equilibrium" (Figure 4, eq 1). The equilibrium is shifted toward hydroxylamine by slow decay of the ascorbate radical via a known multistep mechanism.[13b,24] Addition of reduced glutathione (GSH), which is known to scavenge the ascorbate radical with $k \approx 10$ M^{-1} s^{-1} or dehydroascorbate (disproportionation product of ascorbate radical),[13b,24,25] leads to

(19) Babič, A.; Pečar, S. *Synlett* **2008**, 1155–1158.
(20) X-ray structure of **17** is described in the SI.
(21) Frisch, M. J. et al. *Gaussian 09*, revision A.01; Gaussian: Wallingford, CT, 2009.
(22) Computed ^{1}H hyperfine splitting within each *syn* methyl averages to $|a_H| \approx 0.5$ G. All other *gem*-dimethyls have significantly smaller values of average $|a_H|$ (Table S9, SI).
(23) Vianello, F.; Momo, F.; Scarpa, M.; Rigo, A. *Magn. Reson. Imaging* **1995**, *13*, 219–226.
(24) Bielski, B. H. J.; Allen, A. O.; Schwarz, H. A. *J. Am. Chem. Soc.* **1981**, *103*, 3516–3518.
(25) Winkler, B. S.; Orselli, S. M.; Rex, T. S. *Free Radical Biol. Med.* **1994**, *17*, 333–349.

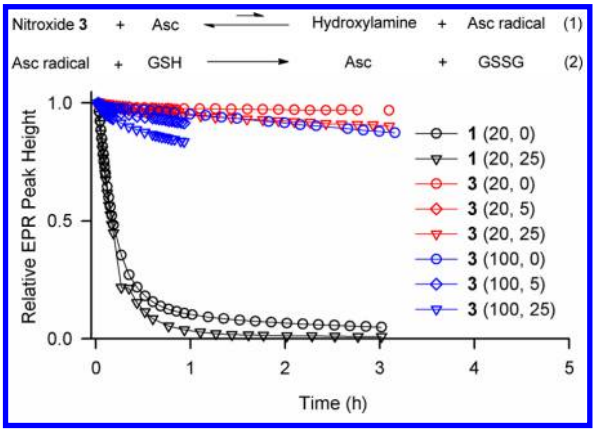

Figure 4. Reduction profiles of 1.0 mM nitroxides in 125 mM PBS pH 7.4 at 295 K. Concentrations of ascorbate (20 or 100 mM) and GSH (0, 5, or 25 mM) are indicated for each experiment.

higher conversion of nitroxide to hydroxylamine. This effect is more pronounced at higher concentrations of ascorbate (Figure 4). In the absence of ascorbate, GSH does not reduce stable nitroxides (Figure S5, SI), and the initial rates of the reduction of studied nitroxides with ascorbate are only slightly increased by the addition of GSH (Table S6, SI).

The slow rate of reduction of **3** compared to that of **2** may be related to increased steric shielding of the nitroxide moiety by *gem*-diethyl vs spirocyclohexyl groups, as shown by the space-filling plots of the X-ray structures (Figure 5).

For further insight into the structure of five-membered ring nitroxides, geometries of **1**–**3** were optimized at the UB3LYP/6-311+G(d,p)+ZPVE level of theory;[21] for **4**–**6**, simplified structures for *cis* and *trans* diastereomers,

(26) Space-filling plots suggest that α-alkylation of the malonate moiety in the *cis* isomer of **4**–**6** may significantly increase steric shielding of nitroxide moiety.

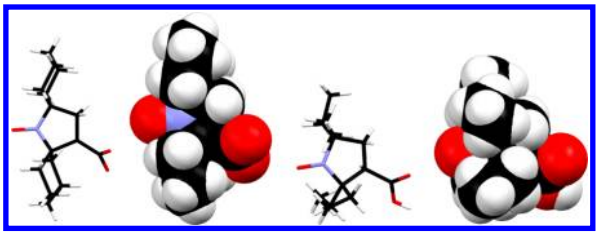

Figure 5. Stick and space-filling plots for X-structures of **2** (left) and **3** (right). Carbon, nitrogen, and oxygen atoms are colored in black, blue, and red, respectively.

in which the diethylmalonate moiety is replaced with a methyl group, are computed at the same level of theory. Space-filling plots for these DFT-computed nitroxides suggest that steric shielding of the nitroxide moiety increases from *gem*-dimethyl to spirocyclohexyl to *gem*-diethyl (Figure S6, SI). Also, steric shielding is more effective in **1**–**3**, compared to the simplified structures of **4**–**6** (Figure S7, SI).[26] Thus, the experimentally observed rate constants for reduction of **1**–**6** by ascorbate may be qualitatively correlated with steric shielding of the NO moiety in pyrrolidine nitroxides.

Acknowledgment. We thank the National Science Foundation and National Institutes of Health for support of this work through Grants CHE-1012578 and NIBIB EB008484. We thank Molly Sowers for her help with the synthesis of **3**.

Supporting Information Available. Complete acknowledgment, ref 21, experimental and computational details, and CIF files. This material is available free of charge via the Internet at http://pubs.acs.org.

The authors declare no competing financial interest.